Science of the Total Environment 735 (2020) 139543

Contents lists available at ScienceDirect

Science of the Total Environment

journal homepage: www.elsevier.com/locate/scitotenv

Species range shifts in response to climate change and human pressure for the world's largest amphibian

Peng Zhang [a,b,*], Xianghong Dong [b,d], Gaël Grenouillet [b,c], Sovan Lek [b], Yichen Zheng [a], Jianbo Chang [a,**]

[a] State Key Laboratory of Water Resources and Hydropower Engineering Science, Wuhan University, Wuhan 430072, China
[b] UMR Laboratoire Evolution et Diversité Biologique, UPS, Toulouse 31062, France
[c] Institut Universitaire de France, Paris 75231, France
[d] State Key Laboratory of Freshwater Ecology and Biotechnology, Institute of Hydrobiology, Chinese Academy of Sciences, Wuhan 430072, China

HIGHLIGHTS

- The species range was predicted using ensemble species distribution modeling.
- Both climate change and human population change would reduce the species range.
- Human pressure is responsible for 71.4% of the range loss and fragment the range.
- Over half of the reserves might lose suitable habitat under the combined impacts.
- Specific mitigation strategies for different reserves should be developed.

GRAPHICAL ABSTRACT

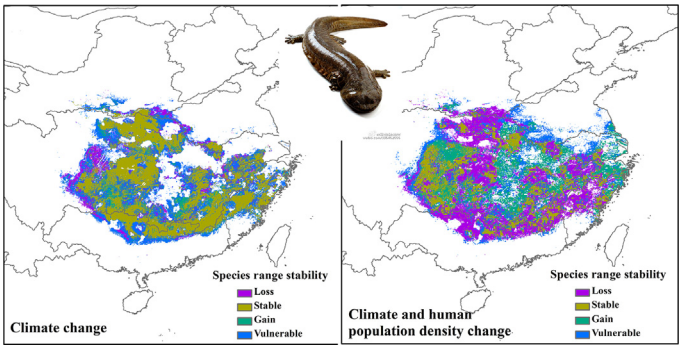

ARTICLE INFO

Article history:
Received 28 February 2020
Received in revised form 17 May 2020
Accepted 17 May 2020
Available online 20 May 2020

Editor: Sergi Sabater

Keywords:
Range loss
Chinese giant salamander
Human population density
Climate change
Species distribution model
Nature reserve

ABSTRACT

The Chinese giant salamander, *Andrias davidianus*, the world's largest amphibian, is critically endangered and has an extremely unique evolutionary history. Therefore, this species represents a global conservation priority and will be impacted by future climate and human pressures. Understanding the range and response to environmental change of this species is a priority for the identification of targeted conservation activities. We projected future range shifts of the Chinese giant salamander under the independent and combined impacts of climate change and human population density (HPD) variations by using ensemble species distribution models. We further evaluated the sustainability of existing nature reserves and identified priority areas for the mitigation or prevention of such pressures. Both climate change and increasing HPD tended to reduce the species range, with the latter leading to greater range losses and fragmentation of the range. Notably, 65.6%, 18.0% and 18.4% of the range loss were attributed solely to HPD change, solely to climate change and to their overlapping impacts, respectively. Overall, the average total and net losses of the species range were 52.5% and 23.4%, respectively, and HPD and climate changes were responsible for 71.4% and 28.6% of the net losses, respectively. We investigated the stability of the remaining species range and found that half of the nature reserves are likely vulnerable, with 57.1% and 66.7% of them likely to lose their conservation value in 2050 and 2070, respectively. To effectively protect this salamander, conservation policies should address both pressures simultaneously, especially considering the negative

* Correspondence to: P. Zhang, State Key Laboratory of Water Resources and Hydropower Engineering Science, Wuhan University, Wuhan 430072, China.
** Corresponding author.
E-mail addresses: zhang1230@whu.edu.cn (P. Zhang), changjb@whu.edu.cn (J. Chang).

https://doi.org/10.1016/j.scitotenv.2020.139543

impact of human pressures in both contemporary periods and the near future. The species range shifts over space and time projected by this research could help guide long-term surveys and the sustainable conservation of wild habitats and populations of this ancient and endangered amphibian.

1. Introduction

The species ranges and abundance of wildlife have been declining for centuries in many parts of the world because of habitat fragmentation, degradation and loss due to anthropogenic threats such as land use change (e.g., urbanization and intensive forestry), invasive species, aquatic pollution, and emerging diseases, with amphibians experiencing greater impacts than most other groups (Wake and Vredenburg, 2008; Yan et al., 2018). Climate change represents yet another threat to wild populations, and the current and future effects of climate change are likely to exacerbate existing stressors (Hof et al., 2011). Amphibians are currently considered the most threatened class of vertebrates worldwide, with approximately one-third of all species imperiled (Stuart et al., 2004). Amphibians, specifically salamanders, are particularly vulnerable to the effects of climate change and pressures from human activities due to their restrictive physiological requirements and low vagility (Barrett and Guyer, 2008). Unlike some species that have dispersal capabilities allowing them to track shifting environmental envelopes, amphibians will experience range contractions when parts of their range no longer exhibit climatic patterns suitable for the maintenance of stable populations (Araújo et al., 2006). In addition, with respect to ongoing habitat destruction, the threats of climate change and other possible human pressures likely are not currently apparent; however, they represent the greatest threats to the persistence of populations in the future (Corn, 2005). Therefore, it is necessary to understand how the species ranges of vulnerable amphibians will respond to future perturbations, including both climate change and human pressures, to ensure long-term conservation.

Correlative species distribution models (SDMs) that have practical advantages in predicting the impacts of changing environments (Fraser et al., 2017; Gallego-Zamorano et al., 2020) have been widely used for the conservation management of land, forest, river and marine ecosystems due to their simplicity and flexibility (Growns et al., 2013; Marshall et al., 2014; Booth, 2018; Khoury et al., 2020). For example, SDMs have been used to examine the effects of climate change on the future spatial distribution of protected areas, identify areas of high conservation value for endangered species (Wilson et al., 2011), guide the search for poorly known species (Fois et al., 2018), model the distributions of threatened species in protected areas (Pěknicová and Berchová-Bímová, 2016), predict the invasion risks of alien species in local areas (Bae et al., 2018; Dong et al., 2020) and support multiobjective ecological restoration decisions for endangered species (Fraser et al., 2017). Although the use of SDMs for nonequilibrium species distributions under contemporary climate conditions is sometimes considered precarious (Fitzpatrick and Hargrove, 2009), attempts have been made to reduce modeling uncertainties through novel techniques (Kearney et al., 2010). These techniques include ensemble methods that average across many different modeling approaches (Hao et al., 2019) and data integration methods based on multiple sources (Isaac et al., 2019). To date, SDMs have been widely explored to project the current and future distributions of salamanders in the context of climate change for local conservation efforts (Werner et al., 2013; Lyons and Kozak, 2019). However, research on the combined impacts of future climate change and human pressures, especially in areas where human pressures affect increasingly large regions and where market forces drive the overexploitation of salamanders, is limited.

The Chinese giant salamander, *Andrias davidianus* (CGS), which is the world's largest amphibian and is endemic to China, is categorized as critically endangered on the IUCN Red List and is a priority for international amphibian conservation because of its extremely unique evolutionary history (Isaac et al., 2012). Once thought to be widespread throughout most of China, this species has been declining in the wild because of human-induced habitat destruction and harvesting for luxury food and is currently critically endangered at the national level (Yan et al., 2018). Effective conservation measures, such as the establishment of nature reserves, have been implemented to protect wild populations. However, conservation interventions are hindered by limited range-wide data because this species is difficult to detect, and only site-level data are available for cryptic species that occur across large geographic areas (Chen et al., 2018). Since large-scale surveys remain impossible for this species, SDMs provide promising tools with which to explore the range of the giant salamander, which is considered a priority activity for spatial conservation planning (Isaac et al., 2012). A recent study revealed that future climate change will severely reduce habitat suitability for the CGS (Zhang et al., 2020); however, human pressures that can considerably influence species range shifts (Turvey et al., 2018) were not considered in the modeling work. In the present study, we explored and quantified the combined impacts of future climate change and human pressure on the CGS distribution. The spatial range shifts in response to the independent and superimposed impacts of these factors were mapped and analyzed, and the near-future sustainability of nature reserves was evaluated. This research can provide insight into the conservation management of the world's largest salamander in both the current period and future periods.

2. Methods

2.1. Species occurrence and conservation status

With a length of two meters and weight of 60 kg, the CGS is the largest recognized extant species of amphibian; it is one of three living cryptobranchid species, which diverged from other amphibians during the mid-Jurassic period. Historically, the species was widely distributed throughout most parts of China; however, it currently mainly lives in central and southern China in three major basin systems: the Yellow, Yangtze, and Pearl River basins (Fig. 1). The sharp decline in population size over the past two decades was largely due to the loss of primary habitat and consumption by humans (Chen et al., 2018; Yan et al., 2018). The species was awarded 'Class II' protection under the Chinese Conservation Law in 1988, and it is currently listed as critically endangered by the IUCN and in Appendix I of CITES. As a conservation measure, several municipal, provincial and national nature reserves have been established, and artificial breeding has been encouraged by the government as a possible conservation measure.

In this study, occurrence data were compiled from three resources: (1) the Global Biodiversity Information Facility (GBIF; http://www.data.gbif.org/) data set; (2) an open-source geodatabase that lists the nature reserves in China (https://www.osgeo.cn/data/); and (3) literature that surveyed and reviewed CGS distribution sites (Wen, 2015; Turvey et al., 2018). The time span of these data covers the second half of the 20th century, when the CGS was widely distributed in China, to the early 21st century. After removing duplicate and apparently erroneous presence records (e.g., records outside of China and terrestrial records far from water), 259 records remained, including records in 23 provincial and national reserves (Supporting Information Table S1). To diminish the effect of spatial autocorrelation originating

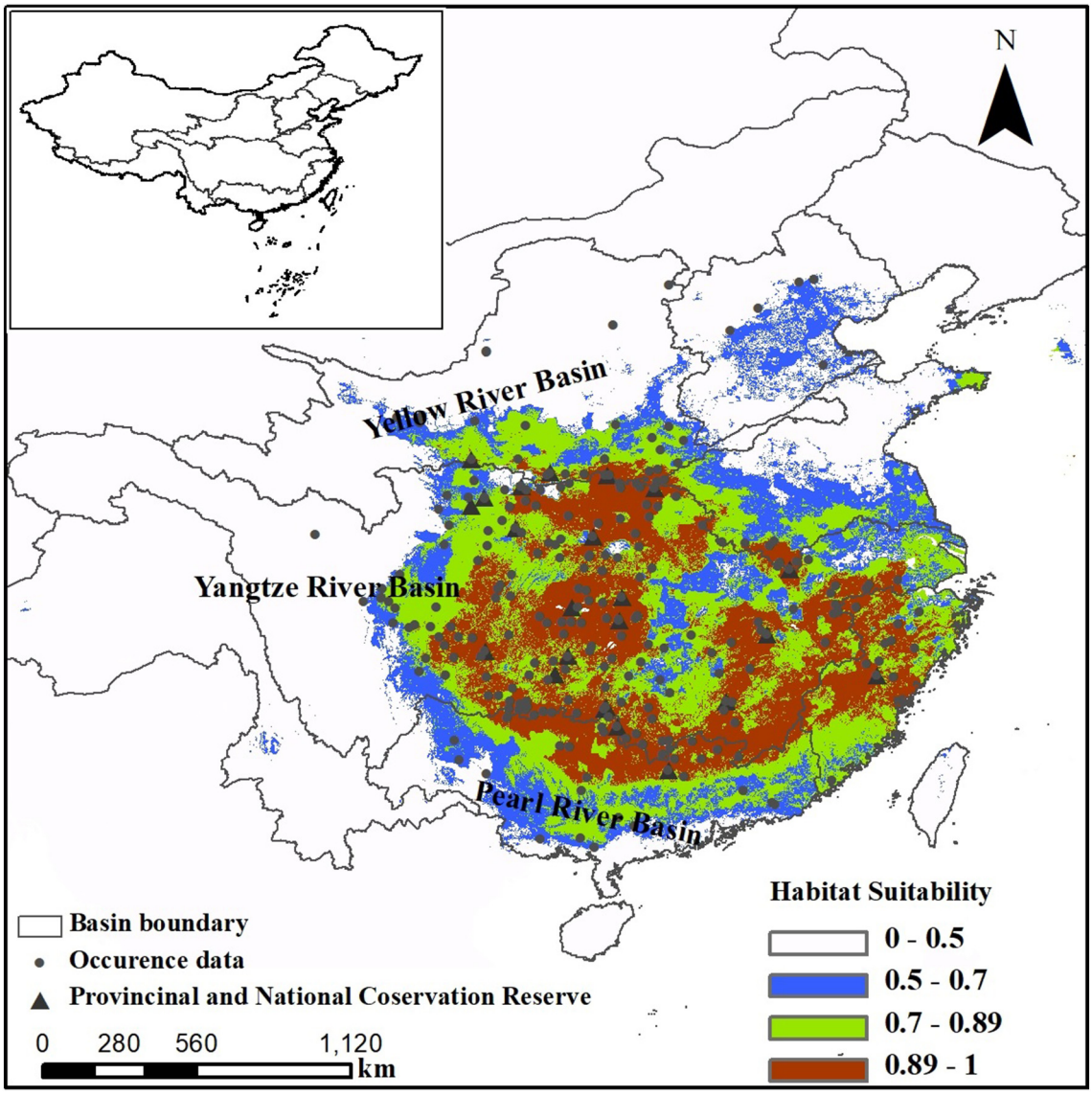

Fig. 1. Locations of provincial and national conservation reserves, occurrence data used for species distribution modeling and the projected current habitat distribution of the CGS.

from the spatial clustering of presence records (i.e., more than one presence record in one environmental grid cell with a 30 arc-second spatial resolution, ca. 1.0 km^2 at the equator), a spatial thinning or rarefying approach similar to that used by Boria et al. (2014) was applied to our presence dataset, selecting at most one record in each environmental grid cell (Feng et al., 2019). Correspondingly, 253 presence records were finally retained. Since presence-absence algorithms are known to perform better than presence-only algorithms (Elith et al., 2006) and true absence records for the CGS at a national scale are impossible to confidently identify, we instead generated 253 pseudo-absence records spanning the whole country and its adjacent areas using a randomization method conditioned by excluding pixels where presences are known (Barbet-Massin et al., 2012). Afterwards, we combined these pseudo-absence records with those retained presence records, and then shuffled the whole dataset to obtain the ultima species presence and pseudo-absence dataset for posterior analysis (Senay et al., 2013).

2.2. Predictor variable selection

The choice of predictor variables can have a strong effect on the quantification of the realized niche and therefore on SDM transferability in time and space (Peterson et al., 2007). We initially selected nineteen climate variables and eleven non-climate variables considered ecologically meaningful for the spatial distribution of this species as candidate predictors (Table 1). The climate variables are commonly used bioclimatic variables (BIO1-BIO19) in the field of ecological niche modeling (Hijmans et al., 2005) from the WorldClim database (http://www.world clim.org), including eleven temperature-related variables and eight precipitation-related variables. The eleven nonclimate variables were land environmental and human-related factors, including land elevation (LAE), waterbody area (WTA), flood hazard frequency (FHF), cropland area (CLA), development pressure index (DPI), human population density (HPD), human population count (HPC), human influence index (HII), human impervious area percentage (HIP), river fragmentation index (RFI), and dam density (DD). Detailed information about these data can be accessed through the sources provided in Table 1. We used two steps to select the predictor variables. First, the variance inflation factor (*VIF*) for each candidate predictor variable was calculated, and the predictor variables with *VIF* values greater than 10 were removed to avoid overfitting and eliminate the effects of collinearity (De Marco and Júnior, 2018). Based on this criterion, fifteen climate variables and two non-climate variables, LAE and HPC, were excluded, with temperature seasonality (BIO4, TS), mean temperature in the coldest

Table 1
Description of tested and selected variables with the selection and exclusion criteria. Variables in bold font were selected for projection and prediction in this study.

Type	Test variables	Description	Selection/Exclusion criteria	Source
	BIO1	Annual Mean Temperature	Collinearity	https://www.worldclim.org/data/worldclim21.html
	BIO2	Mean Diurnal Range (Mean of Monthly (Max Temp - Min Temp))	Collinearity	https://www.worldclim.org/data/worldclim21.html
	BIO3	Isothermality (BIO2/BIO7) (* 100)	Collinearity	https://www.worldclim.org/data/worldclim21.html
	BIO4	**Temperature Seasonality (Standard Deviation *100)**	**Noncollinear and important**	**https://www.worldclim.org/data/worldclim21.html**
	BIO5	Max Temperature of Warmest Month	Collinearity	https://www.worldclim.org/data/worldclim21.html
	BIO6	Min Temperature of Coldest Month	Collinearity	https://www.worldclim.org/data/worldclim21.html
	BIO7	Temperature Annual Range (BIO5-BIO6)	Collinearity	https://www.worldclim.org/data/worldclim21.html
	BIO8	Mean Temperature of Wettest Quarter	Collinearity	https://www.worldclim.org/data/worldclim21.html
	BIO9	Mean Temperature of Driest Quarter	Collinearity	https://www.worldclim.org/data/worldclim21.html
	BIO10	Mean Temperature of Warmest Quarter	Collinearity	https://www.worldclim.org/data/worldclim21.html
	BIO11	**Mean Temperature of Coldest Quarter**	**Noncollinear and important**	**https://www.worldclim.org/data/worldclim21.html**
	BIO12	Annual Precipitation	Collinearity	https://www.worldclim.org/data/worldclim21.html
	BIO13	Precipitation of Wettest Month	Collinearity	https://www.worldclim.org/data/worldclim21.html
	BIO14	Precipitation of Driest Month	Collinearity	https://www.worldclim.org/data/worldclim21.html
	BIO15	**Precipitation Seasonality (Coefficient of Variation)**	**Noncollinear and important**	**https://www.worldclim.org/data/worldclim21.html**
	BIO16	Precipitation of Wettest Quarter	Collinearity	https://www.worldclim.org/data/worldclim21.html
	BIO17	Precipitation of Driest Quarter	Collinearity	https://www.worldclim.org/data/worldclim21.html
	BIO18	**Precipitation of Warmest Quarter**	**Noncollinear and important**	**https://www.worldclim.org/data/worldclim21.html**
Climate	BIO19	Precipitation of Coldest Quarter	Collinearity	https://www.worldclim.org/data/worldclim21.html
	LAE	Land Elevation, extracted from STRM DEM	Collinearity	http://srtm.csi.cgiar.org/download
	WTA	**Waterbody Area**	**Noncollinear and important**	**http://sedac.ciesin.columbia.edu/data/sets/browse**
	FHF	Flood Hazard Frequency	Unimportant	http://sedac.ciesin.columbia.edu/data/sets/browse
	CLA	Cropland Area	Unimportant	http://sedac.ciesin.columbia.edu/data/sets/browse
	DPI	Development Pressure Index	Unimportant	http://sedac.ciesin.columbia.edu/data/sets/browse
	HPD	**Human Population Density**	**Noncollinear and important**	**http://sedac.ciesin.columbia.edu/data/sets/browse**
	HPC	Human Population Count	Collinearity	http://sedac.ciesin.columbia.edu/data/sets/browse
	HII	Human Influence Index	Unimportant	http://sedac.ciesin.columbia.edu/data/sets/browse
	HIP	**Human Impervious Area Percentage**	**Noncollinear and important**	**http://sedac.ciesin.columbia.edu/data/sets/browse**
	DD	Dam Density	Unreasonable	http://www.riverthreat.net/data.html
Nonclimate	RFI	River Fragmentation Index	Unreasonable	http://www.riverthreat.net/data.html

quarter (BIO11, MTCQ), precipitation seasonality (BIO15, PS), precipitation in the warmest quarter (BIO18, PWQ) and other nonclimate variables retained for further selection. Then, we performed an initial round of modeling using the remaining variables and checked the contribution and the shape of the response curve of each variable. Based on variable importance and reasonability criteria, the variables were further selected. The variables with contribution less than 0.01 were removed (i.e., FHF, CLA, DPI and HII). However, two variables with high contribution values, RFI and DD, were left out because their response curves showed that they were unreasonably positively correlated with occurrence probability. Consequently, seven variables, namely, TS, MTCQ, PS, PWQ, WTA, HPD and HIP, were finally selected and used for model projection and prediction in the present study.

2.3. Ensemble species distribution modeling and prediction

Ensemble models are often considered superior to single algorithms because their combined framework can reduce the uncertainties of individual algorithms and provide more robust and reliable projections (Grenouillet et al., 2011). We opted to use four different algorithms that have been frequently applied in the field of ecological niche modeling to establish the basal models required by the ensemble model. These algorithms were a generalized linear model (GLM), generalized boosting model (GBM), random forest (RF) model and multiple adaptive regression splines (MARS) model, and all these algorithms were fit using the default settings of the biomod2 package (Thuiller et al., 2009) in the open-source statistical software R 3.6.1. A random 70% of the total presence and absence records were selected as the training set to calibrate the algorithms; the remaining 30% were withheld for evaluating algorithm performance. This process was replicated 10 times to account for individual algorithm variabilities, avoid bias from the dataset split, and add rigor to the results. Model performance was assessed based on two metrics: the area under the receiver operating characteristic curve (AUC) and the true skill statistic (TSS). Basal models with TSS values over 0.75 and AUC values over 0.90 were selected to develop committee-averaged ensemble models and ensure that the developed ensemble model had the optimal predictive ability for occurrence probability (Guisan et al., 2013). The ensemble models were used to predict habitat suitability for the CGS under current climate conditions and the independent and combined impacts of future climate and HPD changes.

We generated projections for the current climate (1950–2000) and future climates for 2050 (average for 2041–2060) and 2070 (average for 2061–2080), the data for which were obtained from WorldClim 1.4 (http://www.world clim.org). The projections were predicted under three representative concentration pathways (RCP 2.6, 4.5 and 8.5) from three widely used global circulation models (GCMs) (BCC-CSM1-1, CCSM4, and MIROCESM-CHEM) in Asia. As no datasets are available for future HIP and WTA, we kept these two variables static in the future predictions. Future HPD was obtained from global downscaled population projection grids at a resolution of 1 km for 2050 and 2070 (Jones and O'Neill, 2016). This dataset is a downscaled version of the Global One-Eighth Degree Population Projection Grids that is both quantitatively and qualitatively consistent with shared socioeconomic pathways (SSPs). SSPs were developed to support future climate and global change research and the IPCC Sixth Assessment Report (AR6) (Gao, 2019).

2.4. Quantifying the impacts on species range shifts

The results of species distribution modeling represent the probabilities of species occurrence or habitat suitability, and they include some noise and background information. However, in conservation and environmental management practices, information presented based on species presence/absence may be more practical than that presented as a probability or suitability. Therefore, a threshold is needed to transform probability or suitability data to presence/absence data (Liu et al., 2005). This study takes the mean value of the predicted probabilities of species presence, which is regarded as biologically meaningful (Cramer, 2003), as the threshold to transform the projected habitat suitability maps to binary maps, with 1 and 0 representing species presence and absence areas, respectively. Species range shifts in response to climate change and HPD change were evaluated by calculating the difference between the species ranges projected for future and current statuses, with the resulting values of 1, 0, and −1 representing species range expansion, retention and loss, respectively. The areas of total range loss (TRL) and total range expansion were calculated by summing the areas of the grids with values of −1 and 1, respectively. Therefore, the TRL change and net range loss (NRL) change relative to the species range area in the current period were calculated by

$$P_{TRL,f} = \frac{\Delta A_{TRL,f}}{A_c} \times 100\% \quad (1)$$

$$P_{NRL,f} = \frac{\Delta A_{TRL,f} - \Delta A_{E,f}}{A_c} \times 100\% \quad (2)$$

where $\Delta A_{TRL,\,f}$ and $\Delta A_{E,\,f}$ are the areas of TRL and range expansion, respectively; $P_{TRL,\,f}$ and $P_{NRL,\,f}$ are the percentages of TRL and NRL, respectively; A_c is the range area in the current period; and the subscript f can be p, c, or pc, which represent future scenarios impacted by only HPD change, only climate change or their combined changes, respectively.

The contributions of the independent and overlapping impacts of HPD and climate change to range loss were calculated by

$$P_{con,p} = \frac{\Delta A_{TRL,p} - \Delta A_{TRL,o}}{\Delta A_{TRL,pc}} = \frac{P_{TRL,p} - P_{TRL,o}}{P_{TRL,pc}} \quad (3)$$

$$P_{con,c} = \frac{\Delta A_{TRL,c} - \Delta A_{TRL,o}}{\Delta A_{TRL,pc}} = \frac{P_{TRL,c} - P_{TRL,o}}{P_{TRL,pc}} \quad (4)$$

$$P_{con,o} = \frac{\Delta A_{TRL,o}}{\Delta A_{TRL,pc}} = \frac{P_{TRL,o}}{P_{TRL,pc}} = \frac{P_{TRL,p} + P_{TRL,c} - P_{TRL,pc}}{P_{TRL,pc}} \quad (5)$$

where $P_{con,\,p}$, $P_{con,\,c}$, and $P_{con,\,pc}$ represent the range loss change that was driven by only HPD change, only climate change and overlapping impacts, respectively, and $\Delta A_{TRL,\,o}$ and $P_{TRL,\,o}$ represent the overlapping TRL and the percentage of the loss that was negatively impacted by both climate change and HPD in the scenario considering the combined impacts, respectively.

The separate overall impacts of HPD change and climate change were evaluated by

$$P_{imp,p} = \frac{\Delta A_{TRL,p} - \Delta A_{E,p}}{\Delta A_{TRL,pc}} - \Delta A_{E,p} = \frac{P_{NRL,p}}{P_{NRL,pc}} \quad (6)$$

$$P_{imp,c} = \frac{\Delta A_{TRL,c} - \Delta A_{E,c}}{\Delta A_{TRL,pc}} - \Delta A_{E,c} = \frac{P_{NRL,c}}{P_{NRL,pc}} \quad (7)$$

where $P_{imp,\,p}$ and $P_{imp,\,c}$ represent the negative impacts of HPD change and climate change on species range loss, respectively.

The stability of each grid area under the impact of climate change with and without HPD change was evaluated by

$$Stability = \begin{array}{l} Loss, N_{loss,f} > N \times 50\% \; Gain, N_{expasion,f} > N \times 50\% \\ Stable, N_{retain,f} \geq N-1 \; Vulnerable, other\ else \end{array} \quad (8)$$

where N is the total number of climate change scenarios ($N = 9$) and N_{loss}, $N_{expansion}$, and N_{retain} represent the numbers of climate change scenarios under which the species range is lost, expands, and is retained in all climate change scenarios, respectively. The grid areas in which no range loss, retention or expansion would occur in over half of the scenarios were regarded as vulnerable to future environmental change. Specifically, the ability of habitats in the provincial and national nature reserves to sustain the presence of this species under the impacts of climate change and human pressures was explored based on the evaluation of the stability of the species range.

Landscape indices were used to evaluate the impacts of climate change and HPD change on species distribution patterns. The dynamics of habitat patterns within a landscape are normally defined as habitat fragmentation, a process whereby a contiguous patch of habitat is transformed into a number of smaller and disjunctive patches (Cumming and Vervier, 2002). We used patch density and edge density to assess range distribution changes for the CGS. These variables are recognized as effect indices with which to evaluate habitat fragmentation (Wang et al., 2014) and are given by (McGarigal et al., 2012)

$$PD = \frac{n}{A} \times 1000$$

$$ED = \frac{\sum_{k=1}^{n} e_k}{A} \times 1000$$

where PD is patch density (/km^2), ED is edge density (m/km^2), A is the total range area (m^2), n is the number of species range patches, and e_k is the total length (m) of edges for the kth patch. As patch density and edge density measure the degrees of range aggregation or conjunction, higher values of both indices represent greater fragmentation of the species range. All of the above calculations were performed in the open-source statistical software R 3.6.1.

3. Results

3.1. Model performance

The predictive ability of the four modeling algorithms was consistently excellent, with AUC values ranging from 0.89 to 0.98 and TSS values ranging from 0.72 to 0.89 for all the basal models (Fig. 2). RF and GBM were the two best predictive algorithms, with median AUCs of 0.952 and 0.948 and TSSs of 0.815 and 0.827, respectively. Among the 40 basal models, 35 models with high AUCs and TSSs were used to develop the ensemble SDMs. The ensemble model surpassed all of the individual algorithms, with the highest AUC and TSS values of 0.98 and 0.86, respectively (Fig. 2).

3.2. Predominant predictors

The model results indicated that MTCQ, HPD, PWQ, and TS were the most predominant factors affecting the range of the CGS, with importance values of 0.288 ± 0.045, 0.249 ± 0.053, 0.186 ± 0.031, and 0.125 ± 0.067, respectively, whereas PS (0.041 ± 0.008), HIP (0.026 ± 0.005) and WTA (0.018 ± 0.004) played less pivotal roles. Notably, the contribution of HPD to the CGS distribution was nearly equivalent to or greater than the contributions of the other climate variables. The shapes of the response curves of different algorithms for the four most important variables were similar to each other (Fig. 3). More

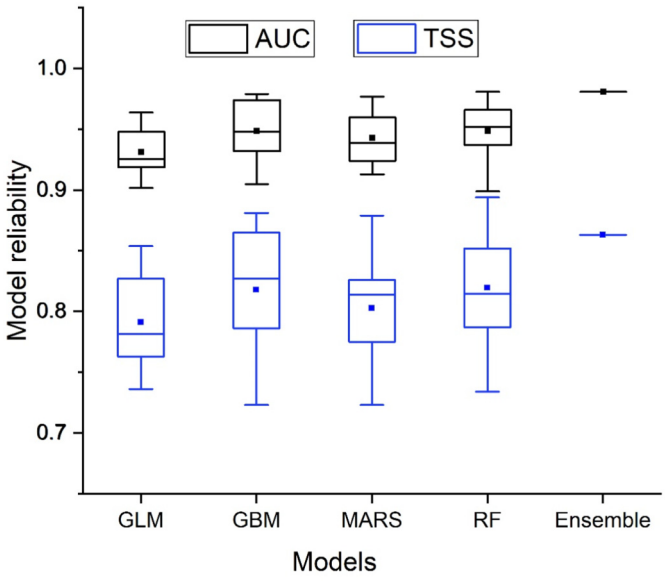

Fig. 2. Model reliability comparison for four machine learning and ensemble modeling methods using AUC and TSS values.

specifically, the occurrence probability of the CGS showed a unimodal response to TS, MTCQ and PWQ, with optimal ranges for the presence of the CGS of approximately 6–10 °C, −4–9 °C and 400–950 mm, respectively. However, occurrence probability showed a decreasing trend with increasing HPD, suggesting that the species distribution is mainly restricted to areas with HPD lower than approximately 400 people per km^2.

3.3. Species distribution shifts

The mean value of suitability based on all the occurrence data calculated from the ensemble model was 0.89, and it was used as the threshold for species presence or absence. The species was shown to be distributed mainly in the Yangtze River Basin (Fig. 1), and the total area of the species range was 1.11×10^6 km^2. The spatial distribution shifts are shown in Fig. 4a-f. In the HPD change scenarios (Fig. 4a, b), the species range obviously expanded toward the north, and a large part of the habitat moved to a previously less suitable area in both 2050 and 2070. The lost distribution areas were widely and discontinuously distributed throughout the area affected by future HPD change. In contrast, both the loss and gain of distribution areas were mainly observed along the internal and external boundaries of the current range under the future climate change scenarios (Fig. 4c, d). Most of the habitat loss occurred in the northern and eastern regions, and habitat expansion mainly occurred in the southern region. Under the combined impacts of climate and HPD changes, the spatial distribution of the losses and gains was similar to that in the solely HPD change scenario, but both the lost and expanded ranges increased (Fig. 4e, f).

Habitat fragmentation analysis showed that the patch density and edge density of the species range obviously increased by 35.7% and 17.7% on average, respectively, in both 2050 and 2070 under the impact of HPD change (Fig. 5). Climate change fragmented the species range, with the patch density and edge density slightly increasing by 8.8% and 3.4%, respectively, on average. Under the combined impacts of HPD and climate changes, species range fragmentation still noticeably increased compared with that under current conditions, despite the edge density being reduced compared with that in the HPD change scenario. These results indicate that although both climate change and HPD change would have negative impacts on the species range of the CGS, HPD change would likely be the dominant factor driving future distribution shifts and range loss.

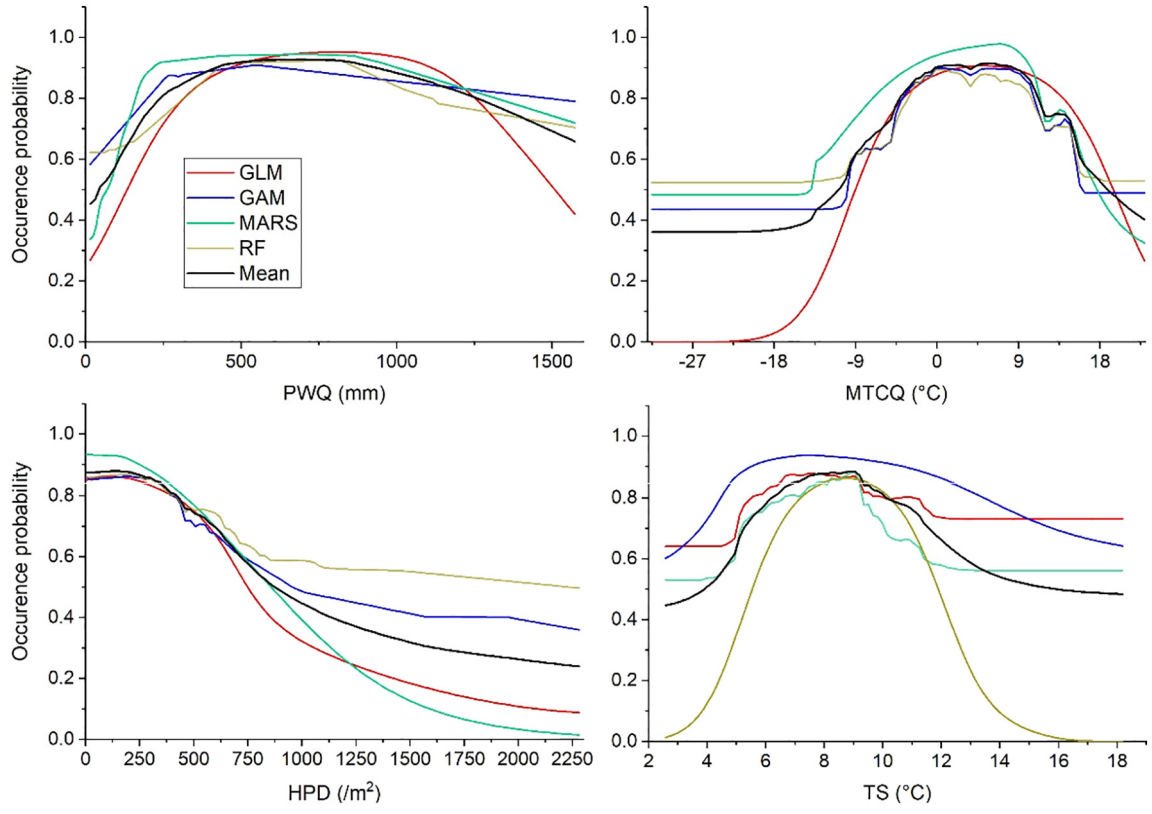

Fig. 3. Response curves for the major predictors.

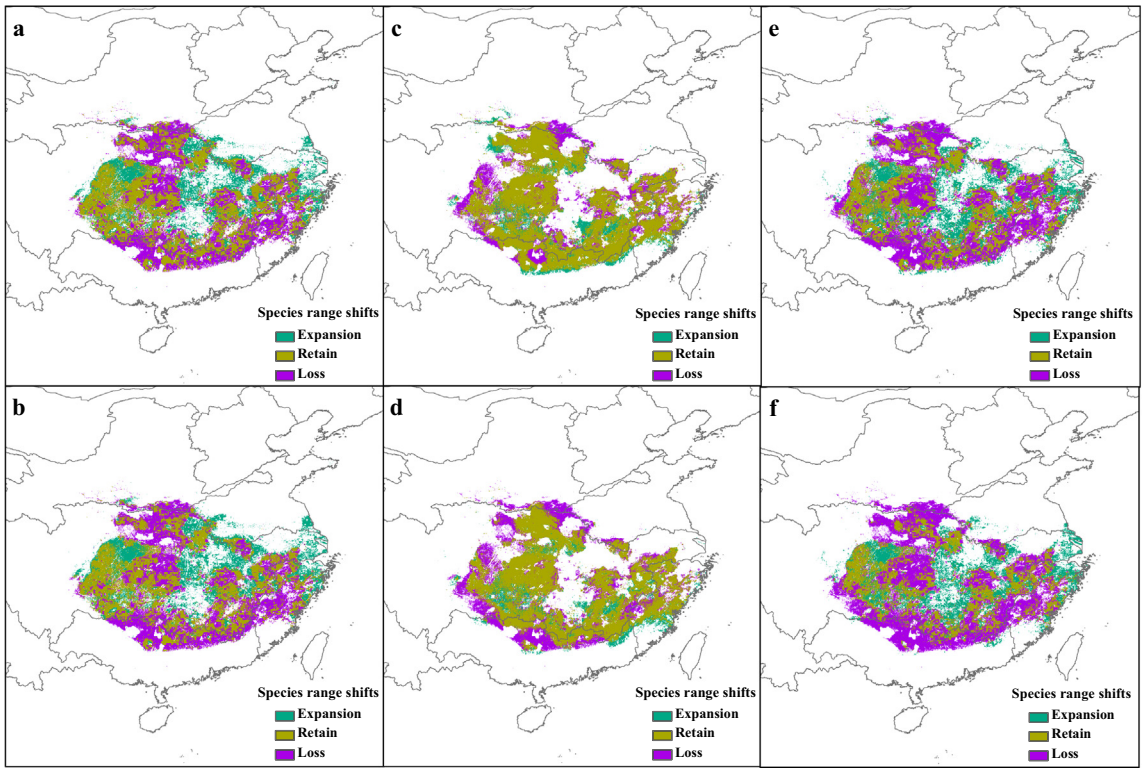

Fig. 4. Shifts in the species range of the CGS under the independent and combined impacts of climate change and HPD change. The scenarios are (a) HPD change in 2050; (b) HPD change in 2070; (c) climate change in 2050; (d) climate change in 2070; (e) HPD and climate change in 2050; and (f) HPD and climate change in 2070.

3.4. Species range loss

Although some gains in the species range were observed under all scenarios, overall reductions were identified throughout the area. Table 2 shows the average percentages of TRL and NRL, combined impacts of climate and HPD changes in 2050 and 2070 (the range losses under all scenarios are shown in Supplementary Table S2). The TRL and NRL exhibit a slight increase in 2070 compared with 2050 under the impact of HPD change. Compared to current conditions, HPD change would lead to a significant reduction in the species range, with the mean percentage of TRL being 44.2% in the two periods. Although the species range would increase in some regions (Fig. 4a, b), the negative impacts of HPD change would dominate, ultimately with an average NRL of 16.7% in 2050 and 2070.

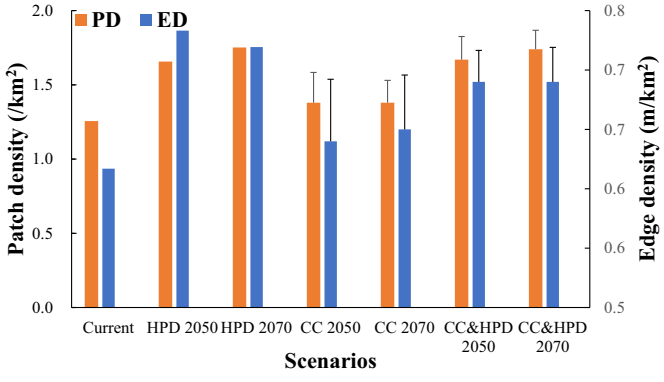

Fig. 5. Comparison of habitat fragmentation indices between different scenarios (PD: patch density, ED: edge density).

Generally, both TRL and NRL in the HPD change scenarios were higher than those in the climate change scenarios (18.1% and 6.7% on average for TRL and NRL, respectively), indicating that HPD change would likely have a more negative impact on the species range. Aggravated loss of the species range was observed under the combined impacts of HPD and climate changes (52.5% on average for TRL). However, 9.7% of the TRL would result from the overlapping effect of HPD and climate changes. Under the combined impacts of HPD and climate changes, 65.6%, 16.0% and 18.4% of the TRL resulted from solely HPD change, solely climate change and their overlapping impacts (calculated by Eqs. (3)–(5)), respectively. Overall, the NRL decreased by 23.4% with HPD change, and climate change explained 71.4% and 28.6% of this loss (calculated by Eqs. (6)–(7)).

3.5. Stability of nature reserves

The stability maps of the species range under the impacts of climate change with and without HPD changes in 2050 and 2070 are shown in Fig. 6. Climate change results in the loss of habitat along the boundaries, with the discontinuous mixing of vulnerable and newly colonized

Table 2
Changes in the total range loss (TRL) and net range loss (NRL) (%) for the CGS under the independent and combined impacts of human population density (HPD) change and climate change (CC).

Loss type	Scenarios	2050	2070	Mean
Total range loss	HPD	42.3	46.0	44.2
	CC	17.9	18.3	18.1
	Combined	51.0	54.1	52.5
	Overlap	9.2	10.2	9.7
Net range loss	HPD	15.2	18.2	16.7
	CC	7.1	6.2	6.7
	Combined	22.3	24.4	23.4

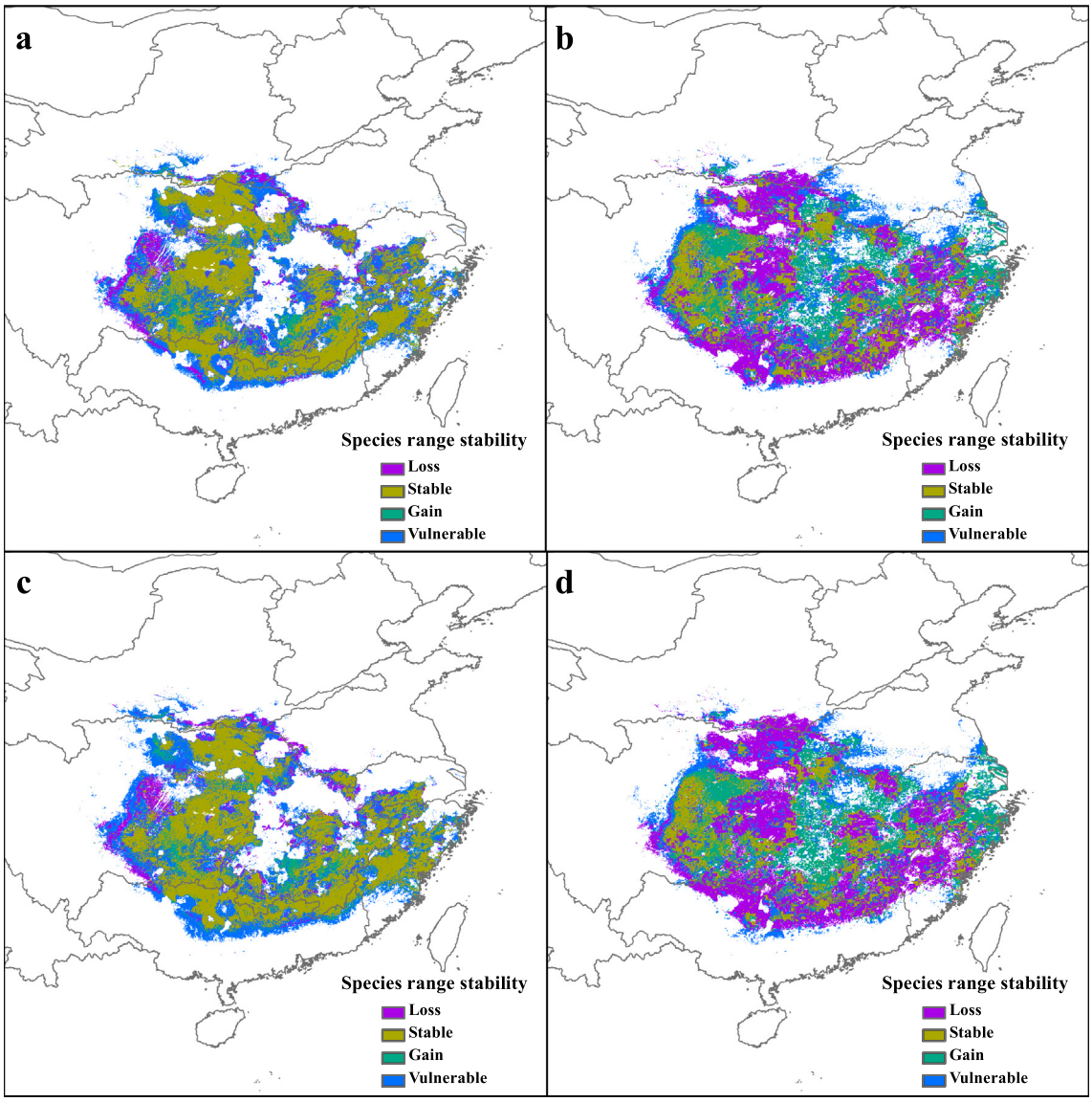

Fig. 6. Species range stability under future scenarios: (a) climate change in 2050; (b) climate change and HPD change in 2050; (c) climate change in 2070; and (d) climate change and HPD change in 2070.

habitats. After integrating the impacts of HPD changes, the extensive stable species range was reduced and fragmented. Based on these maps, the stability of each national and provincial nature reserve site under the independent or combined impacts of HPD and climate changes was evaluated. Habitat stability changes over time and under different scenarios are clearly shown in Table 3. Importantly, two reserves are not recognized as suitable habitat under both current and future environmental conditions. A total of 57.1% of the existing reserves suitable for CGS protection would lose suitable habitat in both 2050 and 2070 in response to future HPD changes. Climate change would cause 23.8% and 28.6% of the reserves to be vulnerable in 2050 and 2070, respectively, and 4.3% and 9.5% of the reserves would lose their habitat. Under the combined impacts of climate and HPD changes, 14.3% of the reserves would become vulnerable and 57.1% and 66.7% of the reserves would likely lose their conservation value in 2050 and 2070, respectively. However, four of the existing reserves would remain stable under the impact of future climate change and HPD change (i.e. Zhangjiajie National Nature Reserve, Xishui National Nature Reserve, Fanjingshan National Nature Reserve, and Luonan Provincial Nature Reserve of CGS).

4. Discussion

4.1. Factors influencing species range shifts

Climate change impacts are likely to be profound for amphibians because they are ectothermic with life cycle and life history attributes that are tightly linked to climate (Bartelt et al., 2010). As ectotherms, amphibians are highly dependent on ambient thermal environments, which influence the physiology, locomotor performance, behavior, habitat use and range-wide distribution of species via their effects on body temperature. This study suggests that the temperature in the coldest quarter and precipitation in the warmest quarter primarily form the climate niche of the CGS. Similar to most amphibians, this species needs to hibernate, which provides protection from cold environments and avoids problems related to food unavailability. Although warming temperatures in winters would provoke earlier emergence from hibernation than usual, increasing temperatures should result in increased energetic expenditure, decreased growth rates, and decreased resource allocation during overwintering periods (Caruso et al., 2014). These pressures from warming winters may drive the species to move toward

Table 3
Stability changes of the CGS reserves under the climate change and HPD change scenarios. S: stable; V: vulnerable; L: lost habitat. The two reserves with bold font do not contain CGS habitatn in current and future conditions, and the four reserves with gray backgrounds would remain stable under future scenarios. Detailed information on the reserves can be found in Supplementary Table S1.

Conservation Reserve ID	HPD change	Climate change		Climate and HPD changes	
	2050/2070	2050	2070	2050	2070
1	L	S	S	L	L
2	L	L	L	L	L
3	L	V	S	L	L
4	L	S	S	L	L
5	L	S	S	L	L
6	S	S	S	S	S
7	L	S	S	V	V
8	L	S	V	L	L
9	S	S	S	V	V
10	S	S	S	S	S
11	S	S	S	S	S
12	S	S	V	S	L
13	S	S	V	V	L
14	L	V	S	L	L
15	S	S	S	L	L
16	L	V	L	L	L
17	L	S	V	L	L
18	**L**	**L**	**L**	**L**	**L**
19	L	S	S	L	L
20	L	V	V	L	L
21	**L**	**L**	**L**	**L**	**L**
22	S	S	S	S	S
23	S	V	V	S	V

cool regions. This species feeds mainly on fish and crustaceans, and its reproductive season is in June and July, when temperatures are warm. As the quantity and temporal patterns of precipitation play an important role in the productivity and species richness of river ecosystems by shaping hydroecological processes (Grimm et al., 2013), sufficient precipitation could provide enough food and a suitable water environment for successful reproduction. Recent research has shown that variation in seasonal climatic conditions also strongly influences the life history, phenology, and geographic location of salamanders (Kirk et al., 2019).

However, our research indicates that future HPD changes will be mainly responsible for the range loss of the CGS. Salamanders possess a variety of characteristics (e.g., cutaneous respiration and low vagility) that make them sensitive to environmental modifications, such as stream alterations and urbanization (Price et al., 2011). The range loss and fragmentation due to HPD changes in both 2050 and 2070 could result from future urban expansion with the economic development of a large number of small and medium-sized cities. As urbanization progresses, land-cover patterns change, and the habitats of species can be destroyed and shrink, especially their wild habitats. The urbanization of catchments not only modifies stream hydrology but also contaminates water (Price et al., 2011), which could expose the species to an unsuitable environment, as it prefers living in fast-flowing and clean water (Chen et al., 2018). In addition, growing human populations are likely to have increased consumption demands for this species, which is widely believed to provide precious nutrients. A deeper impact of future HPD change revealed in this study is habitat fragmentation, which could disrupt movement between formerly contiguous habitats (Marsh et al., 2005), decrease genetic diversity among populations and ultimately contribute to long-term extinction (Noël et al., 2006). The finding that human pressures are primarily responsible for the range losses of the CGS is consistent with the current belief that the decline in the wild population is mostly attributed to overexploitation.

Our study reveals that other two non-climate variables, WTA and HIP, are not most important (variable importance is less than 0.03) for CGS distribution compared with climate variables and HPD. We treated them as unchanging in future prediction as their reliable projections are not available. Actually, the use of static non-climate variables (e.g., slope, soil type and land use/land cover) when predicting climate change impacts in SDM studies is widely accepted (Peterson et al., 2002), and previous work revealed that models including both static variables and dynamic variables perform better than or as well as those either masking or excluding the static variables (Iverson and Prasad, 1998; Stanton et al., 2012). Therefore, although we considered WTA and HIP as static in our study, the future range shifts of the species would be hardly modified. However, it should be noted that if a non-climatic variable is dominate for species distribution, such as HPD in our study, the future dataset should be used in future prediction to

ensure model transferability. In addition, to improve model reliability and thereby model transferability in space and time, selection of model testing and evaluation scheme and spatial autocorrelation checking of the observation and environmental predictors should be particularly concerned. This point is of vital importance not only for presence-only models, but also for presence/absence models used in our study, and should paid more attention in our future work.

4.2. Implications for conservation

The threatened CGS is a global conservation priority, but identification of targeted conservation activities for this species is often impeded by limited baseline data on its status and distribution (Fellowes et al., 2009). Since the 1980s, nature reserves have been established in many provinces to protect wild CGS populations. However, some of the reserves have experienced inefficient management or increased human access to the salamander's habitats (Pan et al., 2015). Our research found that over half of the existing reserves would be unsuitable for the CGS under the combined pressures of climate and HPD changes. If further protection is not implemented, some of the reserves will lose their functionality and value for the conservation of the species. We show the stability shifts of each reserve under the independent impacts of climate change and human pressures (Table 3), and these results could be applied to develop specific mitigation strategies for different reserves to maintain sustainability for the conservation of the CGS. Our study reveals that human pressures will be primarily responsible for the future range losses of this species. This pattern is consistent with the wild population decline being mostly attributed to overexploitation. Therefore, a public information campaign aiming to better educate local inhabitants regarding the status and plight of this important endemic species should be developed, and stricter legislation should be implemented by the government to prohibit the harvesting of wild CGSs. In addition, relevant agencies and bureaus should coordinate and cooperate to ensure effective management. Only in these ways can the largest salamander in the world have long-term and sustainable conservation.

In recent decades, CGS conservation activities have mainly involved the government-supported release of farmed salamanders. However, this strategy may be harmful to wild populations by mixing genetic lineages and spreading pathogens, thereby driving extinction via genetic homogenization (Turvey et al., 2018). Therefore, it is still imperative to enhance conservation strategies to protect the wild habitat and populations of the CGS. The identification of targeted conservation activities for this species is often impeded by limited baseline data on its status and distribution (Fellowes et al., 2009). The species range shifts over space and time predicted by this research could help guide long-term surveys throughout the species' range, detect undiscovered populations and key habitats, understand the life history and genetic evolution of the species, and protect this large and ancient salamander from extinction.

5. Conclusion

This study used a set of SDMs and an ensemble model approach to predict range shifts of the world's largest salamander under the single and combined impacts of future changes in climate and HPD. The results reveal that the ensemble model has the best performance in forecasting the distribution of the CGS and that HPD is almost as important as climate factors in driving the distribution of this endangered species. Future predictions revealed that HPD changes would play the most important role in species range loss and noticeably fragment the habitat compared to the effects of climate change. In addition, over half of the existing nature reserves are likely to lose their suitable habitat under the combined impacts of climate change and HPD change. In light of this, reliable prevention and management strategies should be formulated and implemented, in which lessening the impacts of human-related pressures should be especially addressed. The results provide baseline data that can be used to help protect the wild habitat and populations of this species. Overall, the approach used in this work might provide a valuable reference for research on other endangered species aiming to predict and evaluate future range shifts, especially that on species whose habitat and survival have been strongly affected by human activities.

Article impact statement

Human pressure would contribute 71.4% of range loss and make the habitat fragmented in the future.

CRediT authorship contribution statement

Peng Zhang: Conceptualization, Methodology, Writing - original draft.**Xianghong Dong:**Software, Investigation.**Gaël Grenouillet:**Writing - review & editing, Supervision.**Sovan Lek:**Supervision, Validation. **Yichen Zheng:**Investigation, Visualization.**Jianbo Chang:**Supervision, Project administration.

Declaration of competing interest

The authors declare that they have no known competing financial interests or personal relationships that could have appeared to influence the work reported in this paper.

Acknowledgments

This study was financially supported by the National Natural Science Foundation of China (No. 51709187), the Key Projects in Technology Innovation of Hubei Province, China (No. 2019ACA154) and the China Scholarship Council (CSC). The Evolution et Diversité Biologique laboratory was supported by 'Investissementd'Avenir' grants (CEBA, ref. ANR-10-LABX-0025; TULIP, ref. ANR-10-LABX-41). We thank two anonymous reviewers for their constructive suggestions that greatly improved our work.

Appendix A. Supplementary data

Supplementary data to this article can be found online at https://doi.org/10.1016/j.scitotenv.2020.139543.

References

Araújo, M.B., Thuiller, W., Pearson, R.G., 2006. Climate warming and the decline of amphibians and reptiles in Europe. J. Biogeogr. 33, 1712–1728.
Bae, M.J., Murphy, C.A., Garcia-Berthou, E., 2018. Temperature and hydrologic alteration predict the spread of invasive largemouth bass (Micropterus salmoides). Sci. Total Environ. 639, 58–66.
Barbet-Massin, M., Jiguet, F., Albert, C.H., Thuiller, W., 2012. Selecting pseudo-absences for species distribution models: how, where and how many? Methods Ecol. Evol. 3, 327–338.
Barrett, K., Guyer, C., 2008. Differential responses of amphibians and reptiles in riparian and stream habitats to land use disturbances in western Georgia, USA. Biol. Conserv. 141, 2290–2300.
Bartelt, P.E., Klaver, R.W., Porter, W.P., 2010. Modeling amphibian energetics, habitat suitability, and movements of western toads, Anaxyrus (= Bufo) boreas, across present and future landscapes. Ecol. Model. 221, 2675–2686.
Booth, T.H., 2018. Species distribution modelling tools and databases to assist managing forests under climate change. For. Ecol. Manag. 430, 196–203.
Boria, R.A., Olson, L.E., Goodman, S.M., Anderson, R.P., 2014. Spatial filtering to reduce sampling bias can improve the performance of ecological niche models. Ecol. Model. 275, 73–77.
Caruso, N.M., Sears, M.W., Adams, D.C., Lips, K.R., 2014. Widespread rapid reductions in body size of adult salamanders in response to climate change. Glob. Chang. Biol. 20, 1751–1759.
Chen, S., Cunningham, A.A., Wei, G., Yang, J., Liang, Z., Wang, J., Wu, M., Yan, F., Xiao, H., Harrison, X.A., Pettorelli, N., Turvey, S.T., 2018. Determining threatened species distributions in the face of limited data: spatial conservation prioritization for the Chinese giant salamander (Andrias davidianus). Ecol Evol 8, 3098–3108.
Corn, P.S., 2005. Climate change and amphibians. Anim. Biodivers. Conserv. 28, 59–67.

Cramer, J.S., 2003. Logit Models from Economics and Other Fields. Cambridge University Press.
Cumming, S., Vervier, P., 2002. Statistical models of landscape pattern metrics, with applications to regional scale dynamic forest simulations. Landsc. Ecol. 17, 433–444.
De Marco, P., Júnior, C.C.N., 2018. Evaluating collinearity effects on species distribution models: an approach based on virtual species simulation. PLoS One 13.
Dong, X., Ju, T., Grenouillet, G., Laffaille, P., Lek, S., Liu, J., 2020. Spatial pattern and determinants of global invasion risk of an invasive species, sharpbelly Hemiculter leucisculus (Basilesky, 1855). Sci. Total Environ. 711, 134661.
Elith, J., Graham, C.H., Anderson, R.P., Dudík, M., Ferrier, S., Guisan, A., Hijmans, R.J., Huettmann, F., Leathwick, J.R., Lehmann, A., 2006. Novel methods improve prediction of species' distributions from occurrence data. Ecography 29, 129–151.
Fellowes, J.R., Lau, M.W., Chan, B.P., 2009. Can science in China do more for conservation? Oryx 43, 157–158.
Feng, X., Park, D.S., Liang, Y., Pandey, R., Papeş, M., 2019. Collinearity in ecological niche modeling: confusions and challenges. Ecol. Evol. 9, 10365–10376.
Fitzpatrick, M.C., Hargrove, W.W., 2009. The projection of species distribution models and the problem of non-analog climate. Biodivers. Conserv. 18, 2255.
Fois, M., Cuena-Lombraña, A., Fenu, G., Bacchetta, G., 2018. Using species distribution models at local scale to guide the search of poorly known species: review, methodological issues and future directions. Ecol. Model. 385, 124–132.
Fraser, H., Rumpff, L., Yen, J.D.L., Robinson, D., Wintle, B.A., 2017. Integrated models to support multiobjective ecological restoration decisions. Conserv. Biol. 31, 1418–1427.
Gallego-Zamorano, J., Benitez-Lopez, A., Santini, L., Hilbers, J.P., Huijbregts, M.A.J., Schipper, A.M., 2020. Combined effects of land use and hunting on distributions of tropical mammals. Conserv. Biol. https://doi.org/10.1111/cobi.13459.
Gao, J., 2019. Global Population Projection Grids Based on Shared Socioeconomic Pathways (SSPs), Downscaled 1-km Grids, 2010–2100. NASA Socioeconomic Data and Applications Center (SEDAC), Palisades, NY.
Grenouillet, G., Buisson, L., Casajus, N., Lek, S., 2011. Ensemble modelling of species distribution: the effects of geographical and environmental ranges. Ecography 34, 9–17.
Grimm, N.B., Chapin, F.S., Bierwagen, B., Gonzalez, P., Groffman, P.M., Luo, Y., Melton, F., Nadelhoffer, K., Pairis, A., Raymond, P.A., Schimel, J., Williamson, C.E., 2013. The impacts of climate change on ecosystem structure and function. Front. Ecol. Environ. 11, 474–482.
Growns, I., Rourke, M., Gilligan, D., 2013. Toward river health assessment using species distributional modeling. Ecol. Indic. 29, 138–144.
Guisan, A., Tingley, R., Baumgartner, J.B., Naujokaitis-Lewis, I., Sutcliffe, P.R., Tulloch, A.I., Regan, T.J., Brotons, L., McDonald-Madden, E., Mantyka-Pringle, C., 2013. Predicting species distributions for conservation decisions. Ecol. Lett. 16, 1424–1435.
Hao, T., Elith, J., Guillera-Arroita, G., Lahoz-Monfort, J.J., Serra-Diaz, J., 2019. A review of evidence about use and performance of species distribution modelling ensembles like BIOMOD. Divers. Distrib. 25, 839–852.
Hijmans, R.J., Cameron, S.E., Parra, J.L., Jones, P.G., Jarvis, A., 2005. Very high resolution interpolated climate surfaces for global land areas. International Journal of Climatology: A Journal of the Royal Meteorological Society 25, 1965–1978.
Hof, C., Araújo, M.B., Jetz, W., Rahbek, C., 2011. Additive threats from pathogens, climate and land-use change for global amphibian diversity. Nature 480, 516–519.
Isaac, N.J., Redding, D.W., Meredith, H.M., Safi, K., 2012. Phylogenetically-informed priorities for amphibian conservation. PLoS One 7.
Isaac, N.J.B., Jarzyna, M.A., Keil, P., Dambly, L.I., Boersch-Supan, P.H., Browning, E., Freeman, S.N., Golding, N., Guillera-Arroita, G., Henrys, P.A., Jarvis, S., Lahoz-Monfort, J., Pagel, J., Pescott, O.L., Schmucki, R., Simmonds, E.G., O'Hara, R.B., 2019. Data integration for large-scale models of species distributions. Trends Ecol. Evol. 35, 56–67.
Iverson, L.R., Prasad, A.M., 1998. Predicting abundance of 80 tree species following climate change in the eastern United States. Ecol. Monogr. 68, 465–485.
Jones, B., O'Neill, B.C., 2016. Spatially explicit global population scenarios consistent with the shared socioeconomic pathways. Environ. Res. Lett. 11, 084003.
Kearney, M.R., Wintle, B.A., Porter, W.P., 2010. Correlative and mechanistic models of species distribution provide congruent forecasts under climate change. Conserv. Lett. 3, 203–213.
Khoury, C.K., Carver, D., Barchenger, D.W., Barboza, G.E., Zonneveld, M., Jarret, R., Bohs, L., Kantar, M., Uchanski, M., Mercer, K., Nabhan, G.P., Bosland, P.W., Greene, S.L., Lambrinos, J., 2020. Modelled distributions and conservation status of the wild relatives of Chile peppers (Capsicum L.). Divers. Distrib. 26 (2), 209–225.
Kirk, M.A., Galatowitsch, M.L., Wissinger, S.A., 2019. Seasonal differences in climate change explain a lack of multi-decadal shifts in population characteristics of a pond breeding salamander. PLoS One 14.
Liu, C., Berry, P.M., Dawson, T.P., Pearson, R.G., 2005. Selecting thresholds of occurrence in the prediction of species distributions. Ecography 28, 385–393.
Lyons, M.P., Kozak, K.H., 2019. Vanishing islands in the sky? A comparison of correlation- and mechanism-based forecasts of range dynamics for montane salamanders under climate change. Ecography 0, 1–13.
Marsh, D.M., Milam, G.S., Gorham, N.P., Beckman, N.G., 2005. Forest roads as partial barriers to terrestrial salamander movement. Conserv. Biol. 19, 2004–2008.
Marshall, C.E., Glegg, G.A., Howell, K.L., 2014. Species distribution modelling to support marine conservation planning: the next steps. Mar. Policy 45, 330–332.
McGarigal, K., Cushman, S., Ene, E., 2012. Spatial pattern analysis program for categorical and continuous maps. Computer Software Program Produced by the Authors at the University of Massachusetts, Amherst. FRAGSTATS v4 See. http://wwwumassedu/landeco/research/fragstats/fragstatshtml.
Noël, S., Ouellet, M., Galois, P., Lapointe, F.-J., 2006. Impact of urban fragmentation on the genetic structure of the eastern red-backed salamander. Conserv. Genet. 8, 599–606.
Pan, Y., Wei, G., Cunningham, A.A., Li, S., Chen, S., Milner-Gulland, E.J., Turvey, S.T., 2015. Using local ecological knowledge to assess the status of the critically endangered Chinese giant salamander Andrias davidianus in Guizhou Province, China. Oryx 50, 257–264.
Pěknicová, J., Berchová-Bímová, K., 2016. Application of species distribution models for protected areas threatened by invasive plants. J. Nat. Conserv. 34, 1–7.
Peterson, A.T., Ortega-Huerta, M.A., Bartley, J., Sánchez-Cordero, V., Soberón, J., Buddemeier, R.H., Stockwell, D.R., 2002. Future projections for Mexican faunas under global climate change scenarios. Nature 416, 626–629.
Peterson, A.T., Papeş, M., Eaton, M., 2007. Transferability and model evaluation in ecological niche modeling: a comparison of GARP and Maxent. Ecography 30, 550–560.
Price, S.J., Cecala, K.K., Browne, R.A., Dorcas, M.E., 2011. Effects of urbanization on occupancy of stream salamanders. Conserv. Biol. 25, 547–555.
Senay, S.D., Worner, S.P., Ikeda, T., 2013. Novel three-step pseudo-absence selection technique for improved species distribution modelling. PLoS One 8, e71218.
Stanton, J.C., Pearson, R.G., Horning, N., Ersts, P., Reşit Akçakaya, H., 2012. Combining static and dynamic variables in species distribution models under climate change. Methods Ecol. Evol. 3, 349–357.
Stuart, S.N., Chanson, J.S., Cox, N.A., Young, B.E., Rodrigues, A.S., Fischman, D.L., Waller, R.W., 2004. Status and trends of amphibian declines and extinctions worldwide. Science 306, 1783–1786.
Thuiller, W., Lafourcade, B., Engler, R., Araújo, M.B., 2009. BIOMOD–a platform for ensemble forecasting of species distributions. Ecography 32, 369–373.
Turvey, S.T., Chen, S., Tapley, B., Wei, G., Xie, F., Yan, F., Yang, J., Liang, Z., Tian, H., Wu, M., Okada, S., Wang, J., Lu, J., Zhou, F., Papworth, S.K., Redbond, J., Brown, T., Che, J., Cunningham, A.A., 2018. Imminent extinction in the wild of the world's largest amphibian. Curr. Biol. 28, R592–R594.
Wake, D.B., Vredenburg, V.T., 2008. Are we in the midst of the sixth mass extinction? A view from the world of amphibians. Proc. Natl. Acad. Sci. 105, 11466–11473.
Wang, X., Blanchet, F.G., Koper, N., Tatem, A., 2014. Measuring habitat fragmentation: an evaluation of landscape pattern metrics. Methods Ecol. Evol. 5, 634–646.
Wen, R., 2015. Discussion on the geographical distribution of wild Chinese giant salamander. Hist. Geogr. 86–98.
Werner, P., Lötters, S., Schmidt, B.R., Engler, J.O., Rödder, D., 2013. The role of climate for the range limits of parapatric European land salamanders. Ecography 36, 1127–1137.
Wilson, C.D., Roberts, D., Reid, N., 2011. Applying species distribution modelling to identify areas of high conservation value for endangered species: a case study using Margaritifera margaritifera (L.). Biol. Conserv. 144, 821–829.
Yan, F., Lu, J., Zhang, B., Yuan, Z., Zhao, H., Huang, S., Wei, G., Mi, X., Zou, D., Xu, W., Chen, S., Wang, J., Xie, F., Wu, M., Xiao, H., Liang, Z., Jin, J., Wu, S., Xu, C., Tapley, B., Turvey, S.T., Papenfuss, T.J., Cunningham, A.A., Murphy, R.W., Zhang, Y., Che, J., 2018. The Chinese giant salamander exemplifies the hidden extinction of cryptic species. Curr. Biol. 28, R590–R592.
Zhang, Z., Mammola, S., Liang, Z., Capinha, C., Wei, Q., Wu, Y., Zhou, J., Wang, C., 2020. Future climate change will severely reduce habitat suitability of the critically endangered Chinese giant salamander. Freshw. Biol. 0, 1–10.